STRUCTURAL
BIOLOGY

Volume 78 (2022)

Supporting information for article:

Glycoside hydrolase subfamily GH5_57 features a highly redesigned catalytic interface to process complex hetero-β-mannans

Marcele P. Martins, Mariana A. B. Morais, Gabriela F. Persinoti, Rafael H. Galinari, Li Yu, Yoshihisa Yoshimi, Fernanda Passos Nunes, Tatiani B. Lima, Shayla F. Barbieri, Joana L. M. Silveira, Vincent Lombard, Nicolas Terrapon, Paul Dupree, Bernard Henrissat and Mário T. Murakami

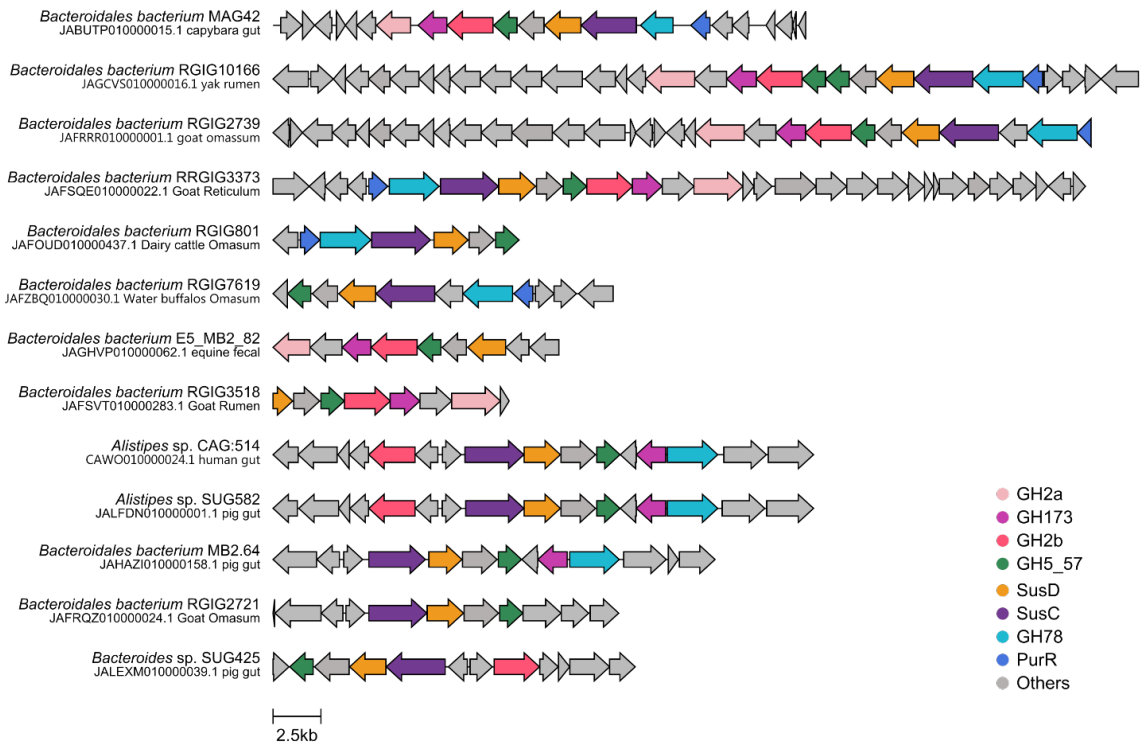

Fig. S1: *Bacteroidales bacterium* MAG42 genomic organization of heteromannan PUL and its conservation in other Bacteroidetes genomes.

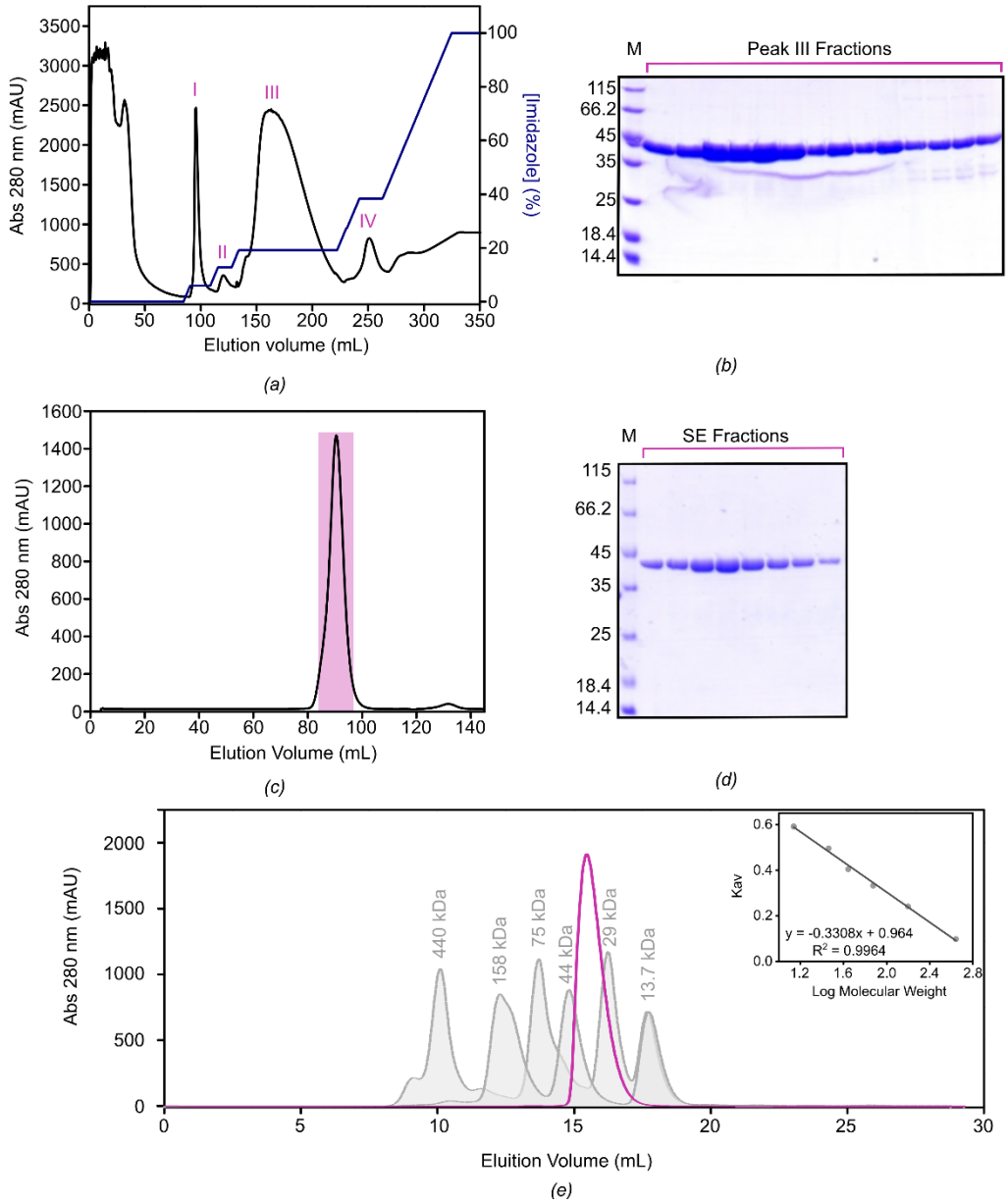

Fig. S2: CapGH5_57 purification. (*a*) Nickel-affinity chromatogram displaying four peaks (I, II, III and IV, highlighted in pink). (*b*) SDS–PAGE analysis of fractions from peak III eluted from affinity chromatography. (*c*) Size-exclusion (SE) chromatogram, highlighting the selected fractions for further experiments (pink rectangle). (*d*) SDS–PAGE analysis of fractions highlighted in (*c*) eluted from size-exclusion chromatography (SE fractions). Lane M, protein molecular weight markers (labelled in kDa). *(e)* Analytic size-exclusion chromatogram of CapGH5_57 (purple line). Molecular weight standards peaks and their respective masses are represented in grey. The CapGH5_57 molecular weight was calculated from the calibration curve using molecular weight standards (*inset*).

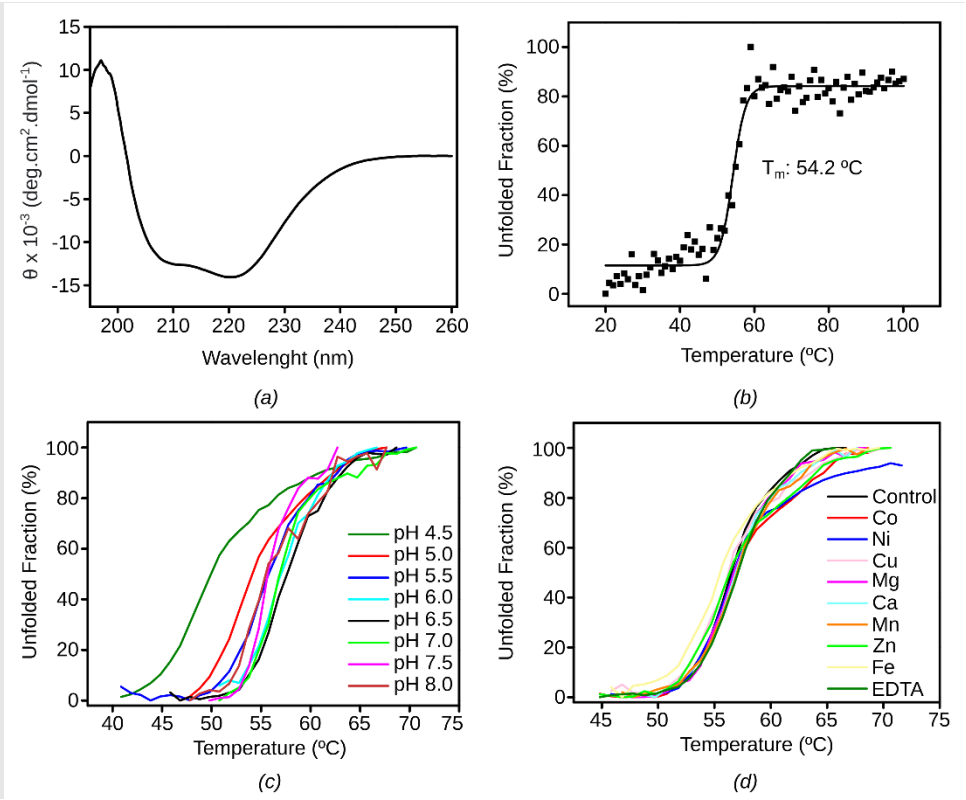

Fig. S3: CapGH5_57 biophysical characterization. (*a*) Circular dichroism spectrum of CapGH5_57. (*b*) CapGH5_57 thermal denaturation profile monitored at 222 nm by circular dichroism spectroscopy. The melting temperature (T_m) was calculated from the sigmoidal fit of the denaturation curve. (*c*) CapGH5_57 differential scanning fluorimetry (DSF) profile with different pH range and (*d*) ions and EDTA.

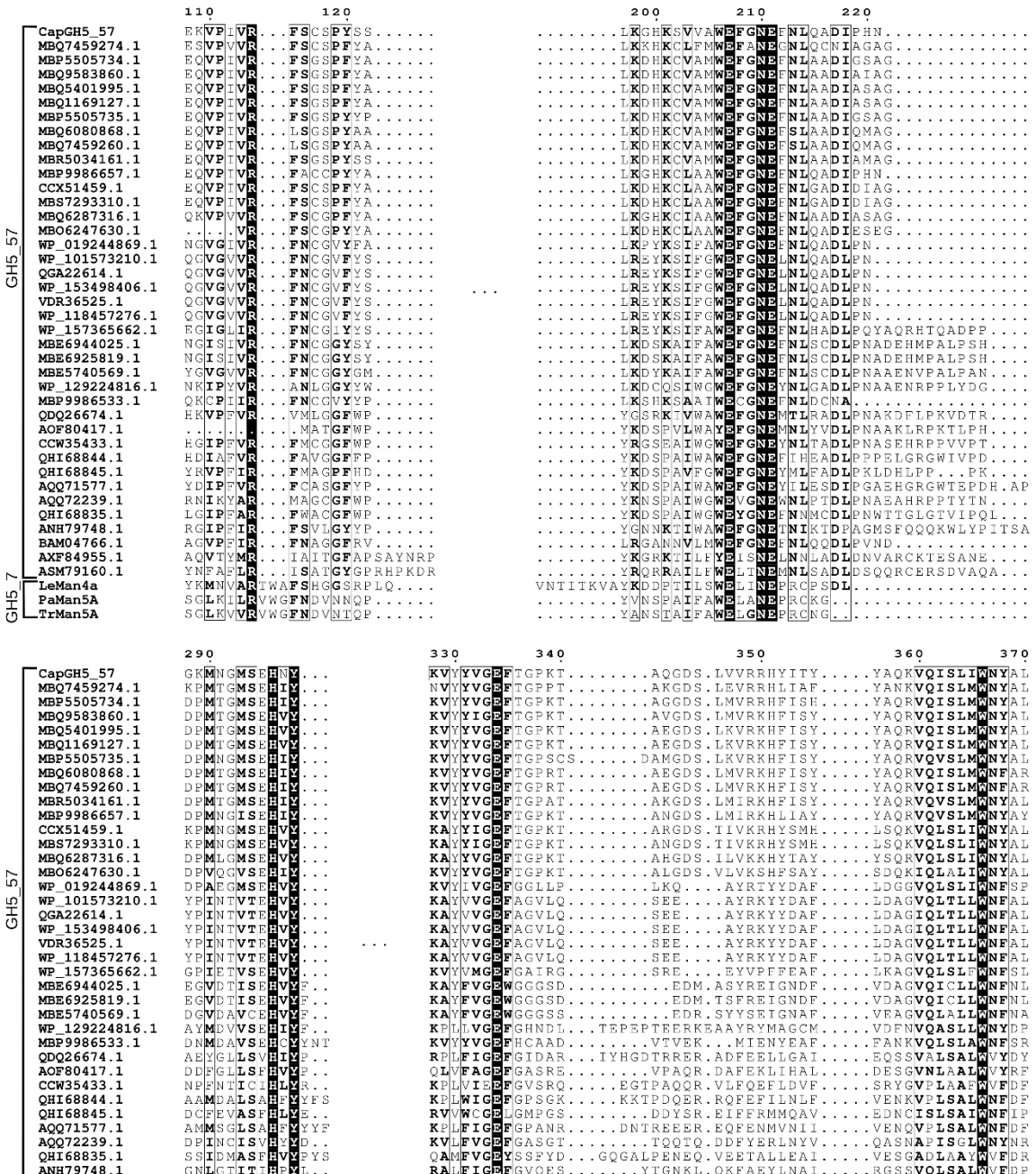

Fig. S4: Multiple sequence alignment of GH5_57 subfamily members and GH5_7 members LeMan4a, PaMan5A and TrMan5A, highlighting the conserved residues. Fully conserved residues of GH5 family are shaded in black (Arg114, Asn210, Glu211, His296, Tyr298, Glu334, and Trp366).

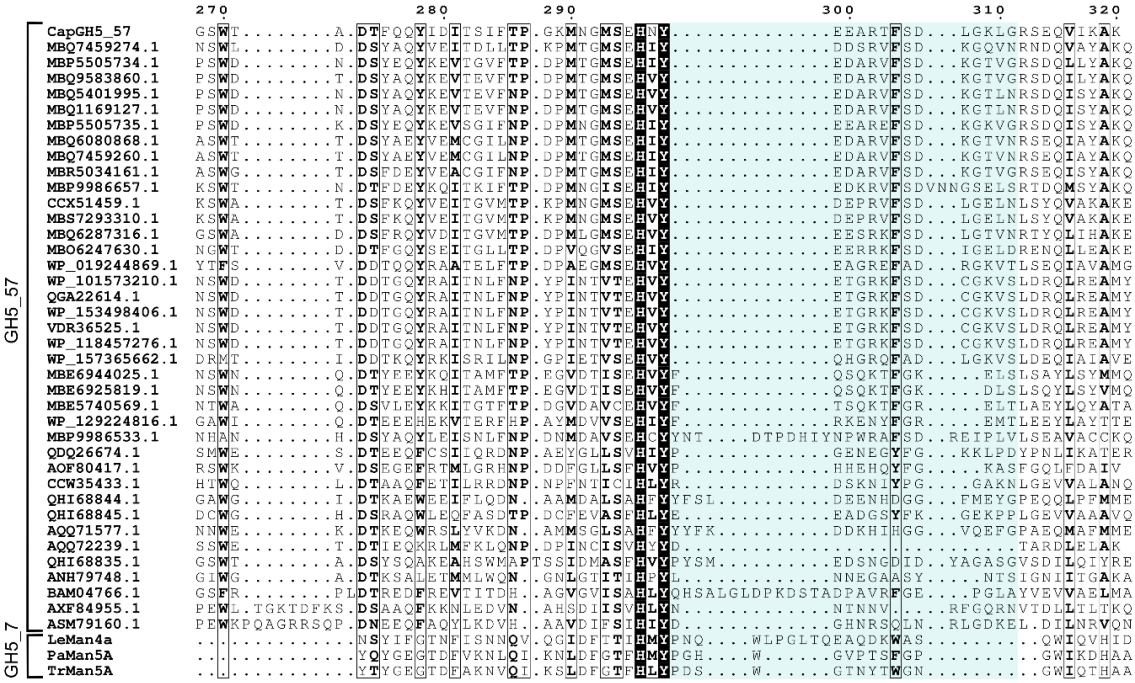

Fig. S5: Multiple sequence alignment of GH5_57 subfamily members and GH5_7 members LeMan4a, PaMan5A and TrMan5A, highlighting the divergent β6-α6 region. Identical residues are shaded in black. The region encompassing the divergent helix ($\alpha6_a$), within the β6-α6 loop (Glu299-Gly311) is highlighted in light blue.

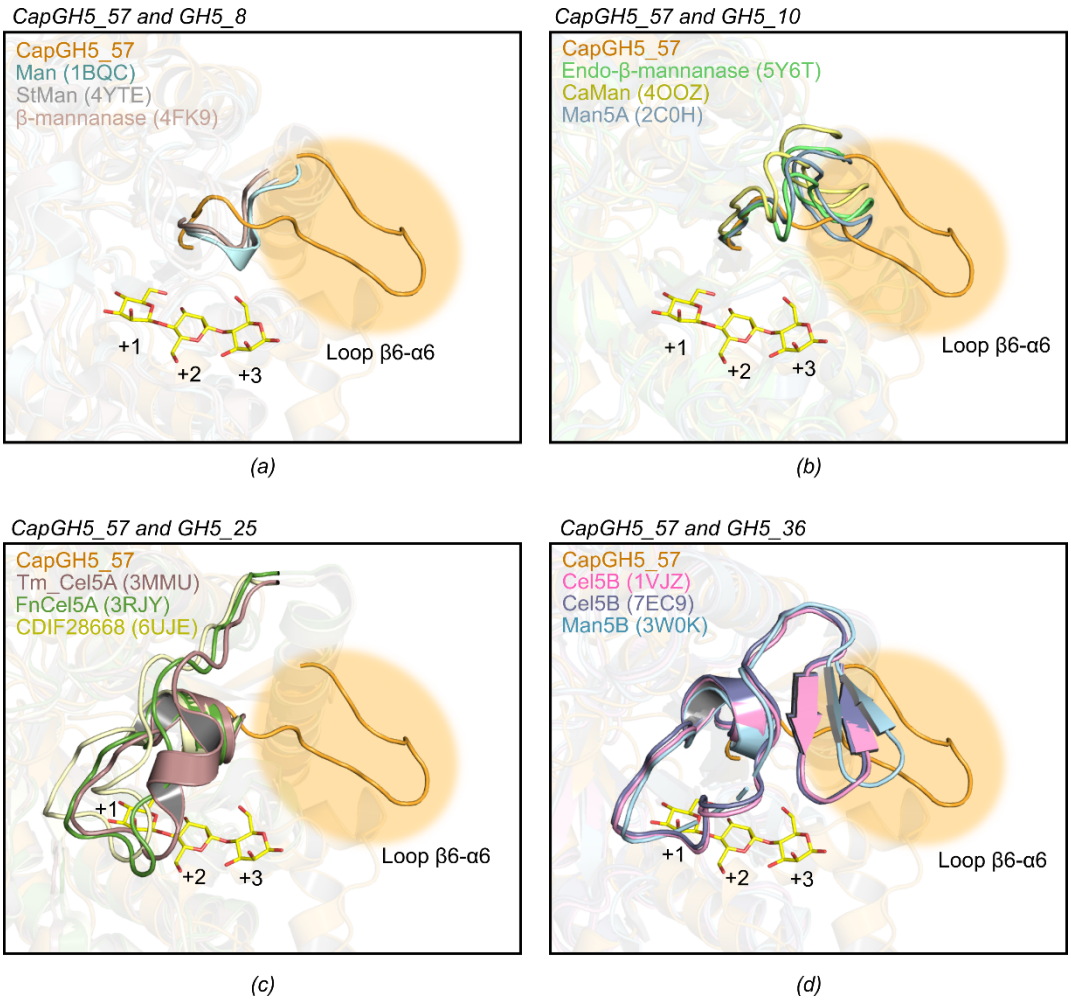

Fig. S6: Structural comparison of CapGH5_57 β6-α6 loop with GH5 subfamilies displaying endo-β-mannanase activity. (*a*) Structural superimposition of CapGH5_57 and GH5_8 (Man PDB code 1BQC (Hilge *et al.*, 1998), StE273Adc PDB code 4Y7E (Kumagai *et al.*, 2015) and β-mannanase PDB code 4FK9 (Takasuka *et al.*, 2014)), (*b*) Structural superimposition of CapGH5_57 and GH5_10 (Endo-β-mannanase PDB code 5Y6T (Ueda *et al.*, 2018), CaMan PDB code 4OOZ (Kim *et al.*, 2014), and Man5A PDB code 2C0H (Larsson *et al.*, 2006)), (*c*) Structural superimposition of CapGH5_57 and GH5_25 (Tm_Cel5A PDB code 3MMU (Pereira *et al.*, 2010), FnCel5A PDB code 3RJY (Zheng *et al.*, 2012), and CDIF28668 PDB code 6UJE (Scott *et al.*, 2020)). (*d*) Structural superimposition CapGH5_57 and GH5_36 (Cel5B PDB codes 1VJZ (Joint Center for Structural Genomics, 2004) and 7EC9 (Manoj & Garg, 2022)) and Man5B PDB code 3W0K (Oyama *et al.*, 2013)). The manno-oligosaccharide (yellow sticks) was extracted from the endo-β-mannanase StE273Adc (PDB code 4Y7E).

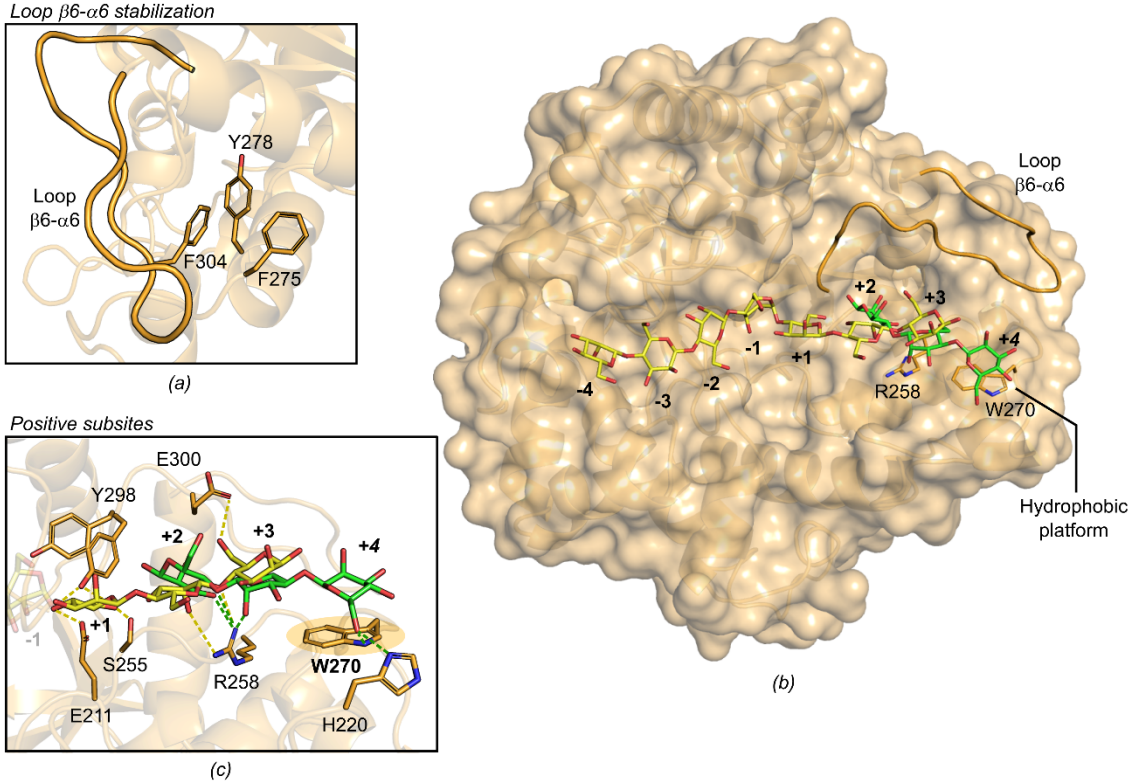

Fig. S7: CapGH5_57 β6-α6 loop stabilization and the hydrophobic platform comprising the distal subsites. (*a*) Representation of aromatic cluster that potentially stabilizes the β6-α6 loop. (*b*) Surface representation with the β6-α6 loop represented in cartoon and the distal positive subsites highlighted (sticks). The manno-oligosaccharide (yellow sticks) was obtained from structural superimposition with endo-β-mannanase StE273Adc (PDB code 4Y7E (Kumagai *et al.*, 2015)). The oligosaccharide represented in green sticks is a fragment of the docked sugar (retrieved from PDB code 4Y7E) in the CapGH5_57 active site (additional sugar units were omitted for clarity). *(c)* Positive subsites interactions with the manno-oligosaccharides described in (*b*). The yellow and green dashed lines represent the interaction of residues with the original (from structural superimposition) and the fragment of the docked oligosaccharide, respectively. The hydrophobic platform at the +4 subsite comprising the Trp270 is highlighted in light orange.

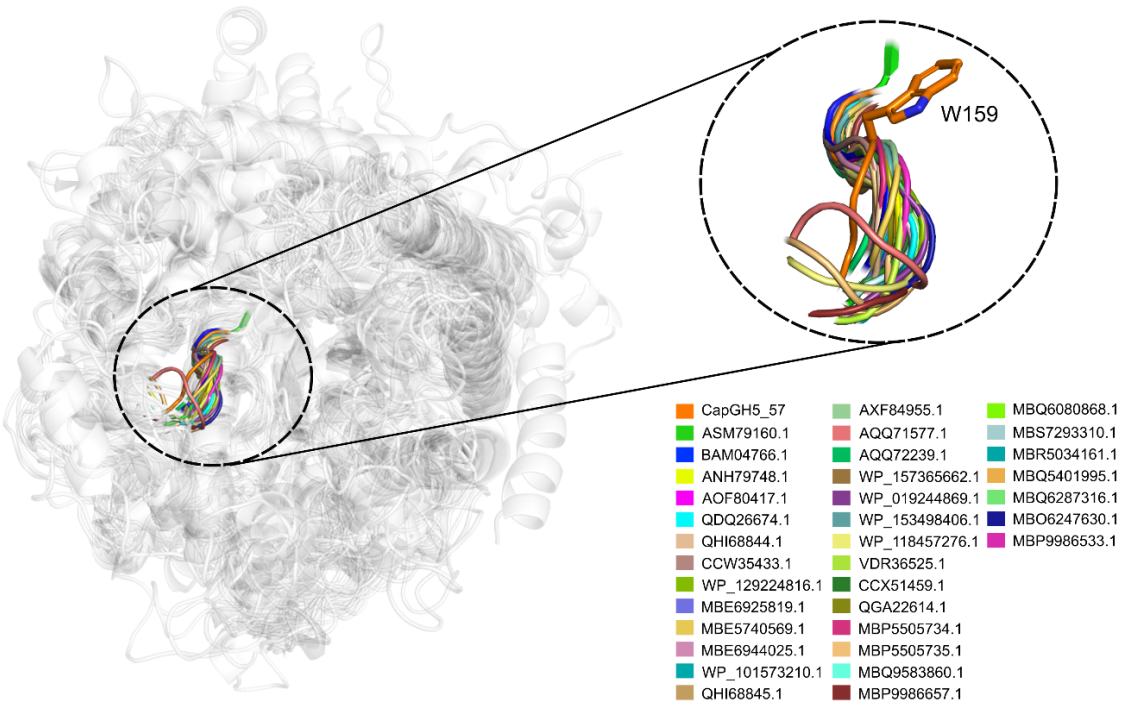

Fig. S8: Structural comparison between CapGH5_57 and the catalytic domain of other GH5_57 members (Table S9), highlighting the loop containing the residue Trp159. All CapGH5_57 orthologues were modeled using RoseTTAFold, available in the Robetta server (Baek *et al.*, 2021). The commands “super or cealign” in the PYMOL were used for structural alignment. The loop shortening is highlighted in the right panel and the name of each member is represented by different colors.

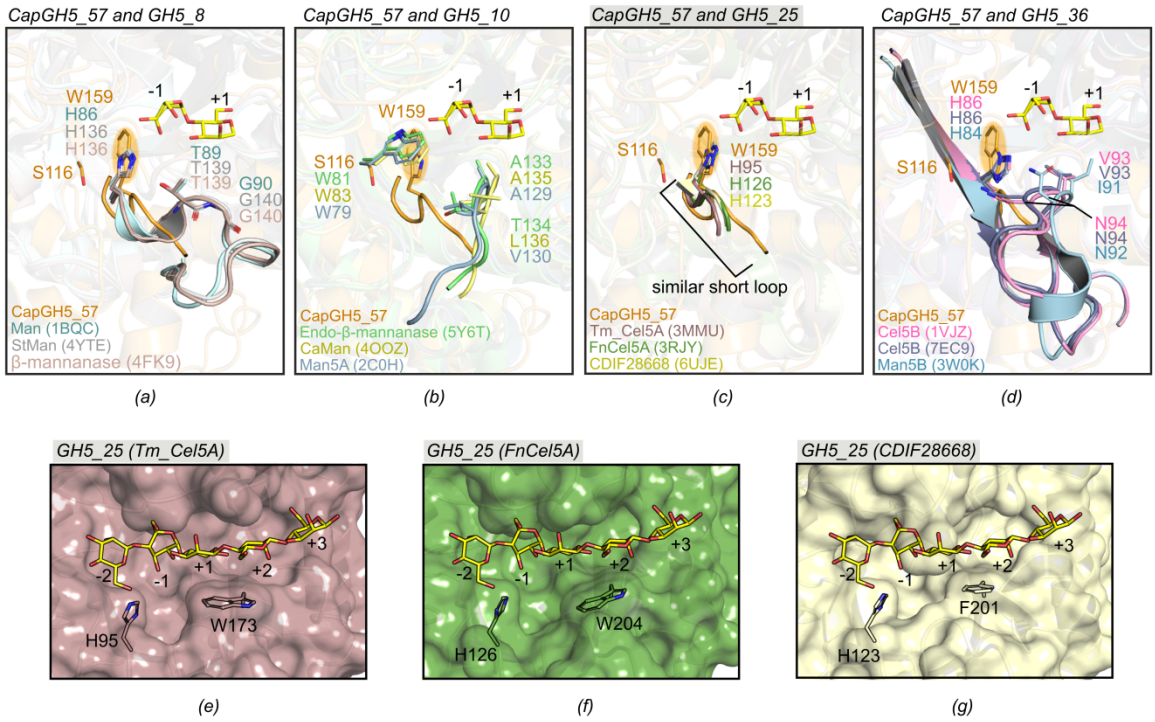

Fig. S9: Structural comparison of the Trp159-containing loop between CapGH5_57 and other GH5 subfamilies displaying endo-β-mannanase activity. Comparison between CapGH5_57 and the three most similar members (according to the DALI server) of the subfamilies (*a*) GH5_8 (Man, PDB code 1BQC (Hilge *et al.*, 1998); StE273Adc, PDB code 4Y7E (Kumagai *et al.*, 2015); and β-mannanase, PDB code 4FK9 (Takasuka *et al.*, 2014)), (*b*) GH5_10 (Endo-β-mannanase, PDB code 5Y6T (Ueda *et al.*, 2018); CaMan, PDB code 4OOZ (Kim *et al.*, 2014); and Man5A, PDB code 2C0H (Larsson *et al.*, 2006)), (*c*) GH5_25 (Tm_Cel5A, PDB code 3MMU (Pereira *et al.*, 2010); FnCel5A, PDB code 3RJY (Zheng *et al.*, 2012); and CDIF28668, PDB code 6UJE (Scott *et al.*, 2020)) and (*d*) GH5_36 (Cel5B, PDB codes 1VJZ (Joint Center for Structural Genomics, 2004) and 7EC9 (Manoj & Garg, 2022); and Man5B, PDB code 3W0K (Oyama *et al.*, 2013)). The manno-oligosaccharide spanning the –1 and +1 subsites was extracted from the GH5_8 endo-β-mannanase StE273Adc (PDB code 4Y7E (Kumagai *et al.*, 2015)). View of the active site of GH5_25 members, highlighting the hydrophobic platform at the +1 subsite from the other β-sheet of (*e*) Tm_Cel5A (PDB code 3MMU), (*f*) FnCel5A (PDB code 3RJY), and (*g*) CDIF28668 (PDB code 6UJE). The manno-oligosaccharide spanning the –2 to +3 subsites was also extracted from endo-β-mannanase StE273Adc (PDB code 4Y7E (Kumagai *et al.*, 2015)).

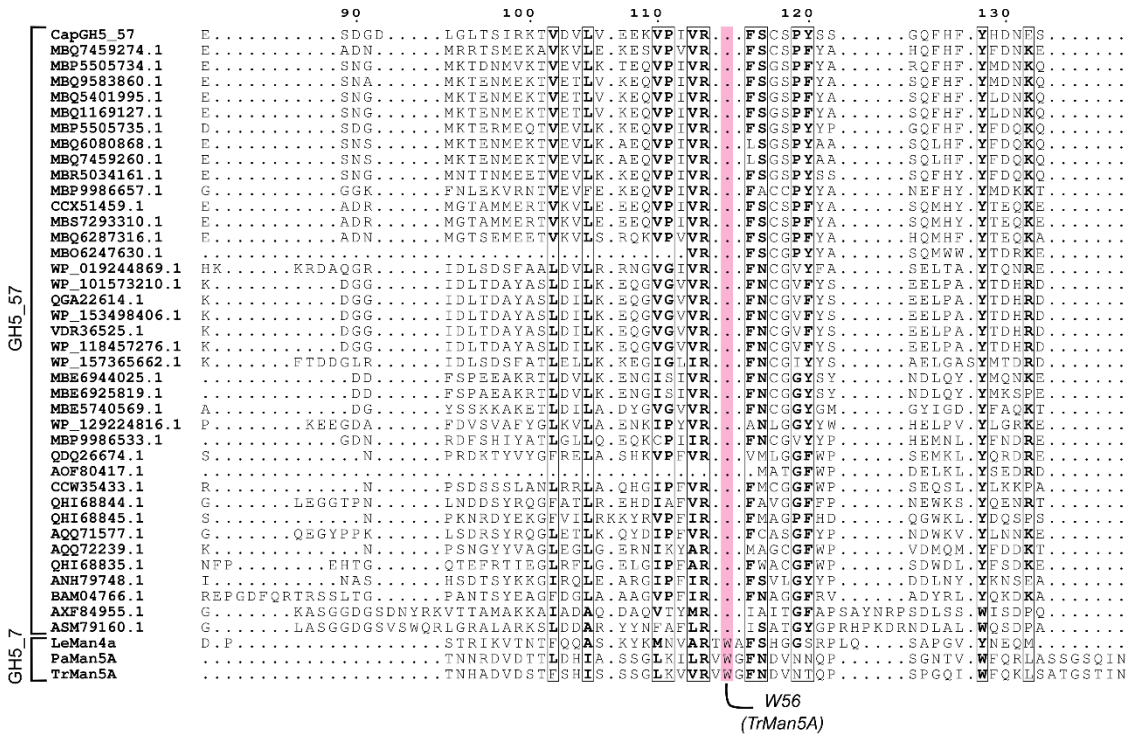

Fig. S10: Multiple sequence alignment of GH5_57 members and characterized GH5_7 members LeMan4a, PaMan5A and TrMan5A, highlighting the Trp conserved in the GH5_7 subfamily, but absent in the GH5_57 subfamily. Conserved residues are highlighted in black. The lack of Trp56 (numbered according to TrMan5A, PDB code 1QNO (Sabini *et al.*, 2000) is highlighted in pink.

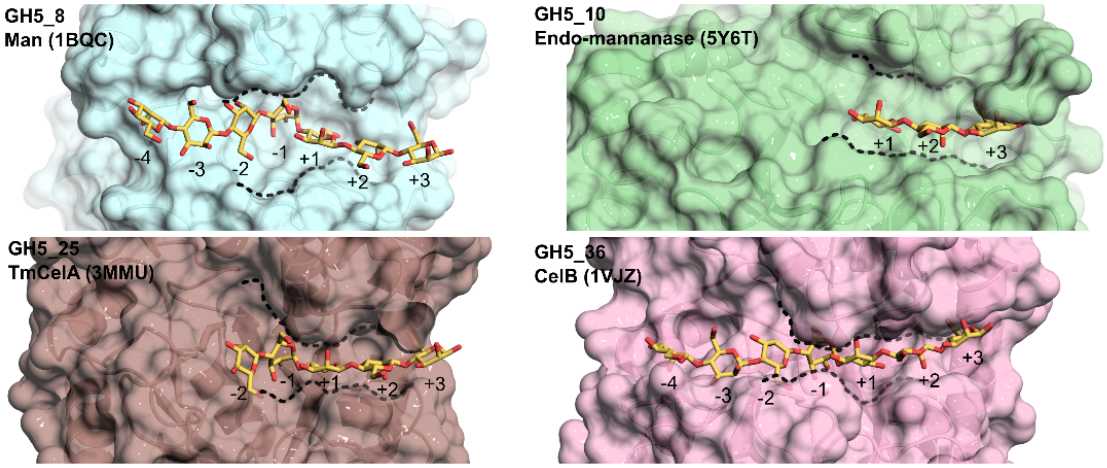

Fig. S11. Overall view of the active site topology of GH5 endo-β-mannanases from subfamilies GH5_8, GH5_10, GH5_25 and GH5_36. The represented structures correspond to the three most similar members (according to the DALI server (Holm, 2022) from subfamilies GH5_8 (Man, PDB code 1BQC (Hilge *et al.*, 1998), cyan surface), GH5_10 (Endo-β-mannanase, PDB code 5Y6T (Ueda *et al.*, 2018), green surface), GH5_25 (TmCel5A, PDB code 3MMU (Pereira *et al.*, 2010), brown surface) and GH5_36 (Cel5B, PDB code 1VJZ, (Joint Center for Structural Genomics, 2004), pink surface). The manno-oligosaccharide fragments (yellow sticks) were extracted from the endo-β-mannanase StE273Adc (PDB code 4Y7E, (Kumagai *et al.*, 2015)).

Supplementary References

Baek, M., DiMaio, F., Anishchenko, I., Dauparas, J., Ovchinnikov, S., Lee, G. R., Wang, J., Cong, Q., Kinch, L. N., Dustin Schaeffer, R., Millán, C., Park, H., Adams, C., Glassman, C. R., DeGiovanni, A., Pereira, J. H., Rodrigues, A. V., Van Dijk, A. A., Ebrecht, A. C., Opperman, D. J., Sagmeister, T., Buhlheller, C., Pavkov-Keller, T., Rathinaswamy, M. K., Dalwadi, U., Yip, C. K., Burke, J. E., Garcia, K. C., Grishin, N. V., Adams, P. D., Read, R. J. & Baker, D. (2021). *Science.* **373**, 871–876.

Hilge, M., Gloor, S. M., Rypniewski, W., Sauer, O., Heightman, T. D., Zimmermann, W., Winterhalter, K. & Piontek, K. (1998). *Structure*. **6**, 1433–1444.

Holm, L. (2022). *Nucleic Acids Res.* **50**, W210–W215.

Joint Center for Structural Genomics (2004). Crystal structure of Endoglucanase (TM1752) from Thermotoga maritima at 2.05 A resolution. doi:10.2210/pdb1VJZ/pdb.

Kim, M. K., An, Y. J., Song, J. M., Jeong, C. S., Kang, M. H., Kwon, K. K., Lee, Y. H. & Cha, S. S. (2014). *Proteins Struct. Funct. Bioinforma.* **82**, 3217–3223.

Kumagai, Y., Yamashita, K., Tagami, T., Uraji, M., Wan, K., Okuyama, M., Yao, M., Kimura, A. & Hatanaka, T. (2015). *FEBS J.* **282**, 4001–4014.

Larsson, A. M., Anderson, L., Xu, B., Muñoz, I. G., Usón, I., Janson, J. C., Stålbrand, H. & Ståhlberg, J. (2006). *J. Mol. Biol.* **357**, 1500–1510.

Manoj, N. & Garg, P. (2022). Structure of the Thermotoga maritima Family 5 endo-glucanase in complex with 1-deoxynojiromycin. doi: 10.2210/pdb7EC9/pdb.

Oyama, T., Schmitz, G. E., Dodd, D., Han, Y., Burnett, A., Nagasawa, N., Mackie, R. I., Nakamura, H., Morikawa, K. & Cann, I. (2013). *PLoS One*. **8**, e80448.

Pereira, J. H., Chen, Z., McAndrew, R. P., Sapra, R., Chhabra, S. R., Sale, K. L., Simmons, B. A. & Adams, P. D. (2010). *J. Struct. Biol.* **172**, 372–379.

Sabini, E., Schubert, H., Murshudov, G., Wilson, K. S., Siika-Aho, M. & Penttilä, M. (2000). *Acta Crystallogr. Sect. D Biol. Crystallogr.* **56**, 3–13.

Scott, W., Lowrance, B., Anderson, A. C. & Weadge, J. T. (2020). *PLoS One*. **15**, e0242686.

Takasuka, T. E., Acheson, J. F., Bianchetti, C. M., Prom, B. M., Bergeman, L. F., Book, A. J., Currie, C. R. & Fox, B. G. (2014). *PLoS One*. **9**, e94166.

Ueda, M., Hirano, Y., Fukuhara, H., Naka, Y., Nakazawa, M., Sakamoto, T., Ogata, Y. & Tamada, T. (2018). *Enzyme Microb. Technol.* **117**, 15–22.

Zheng, B., Yang, W., Zhao, X., Wang, Y., Lou, Z., Rao, Z. & Feng, Y. (2012). *J. Biol. Chem.* **287**, 8336–8346.